Semi-supervised Bayesian Source Separation of Scintigraphic Image Sequences

Lenka Bódiová, Ondřej Tichý, and Václav Šmídl

Abstract Many diagnostic methods using scintigraphic image sequence require decomposition of the sequence into tissue images and their time-activity curves. Standard procedure for this task is still manual selection of regions of interest (ROIs) which can be highly subjective due to their overlaps and poor signal-to-noise ratio. This can be overcome by automatic decomposition, however, the results may not have good physiological meaning. In this contribution, we aim to combine these approaches in semi-supervised procedure which is based on Bayesian blind source separation with the possibility of manual interaction after each run until an acceptable solution is obtained. The manual interaction is based on manul ROI placement and using its position to modify the corresponding prior parameters of the model. Performance of the proposed method is studied on real scintigraphic image sequence as well as on estimation of the specific diagnostic parameter on representative dataset of 10 scintigraphic sequences.

Keywords: Dynamic Renal Scintigraphy, Regions of Interest, Blind Source Separation, Factor Analysis, Variational Bayes Method

1 Introduction

In dynamic scintigraphy, radiopharmaceuticals, i.e. pharmaceutical drugs with radioactivity, are applied into a human body. Subsequently, the emitted gamma radiation is repetitively captured by a scintigraphic camera. By

Lenka Bódiová
Faculty of Nuclear Sciences and Physical Engineering, CTU in Prague, Brehova 7, Czech Republic, e-mail: bodiova.lenka@gmail.com

Ondřej Tichý and Václav Šmídl
Institute of Information Theory and Automation, Prague, Pod Vodarenskou vezi 4, Czech Republic, e-mail: otichy@utia.cas.cz and smidl@utia.cas.cz

doing this, a sequence of images is obtained. By analyzing the sequence, an accumulation and distribution of the radioactive substance in the organ of interest can be studied. Such information is important for examination of the organ's function. In this paper, we will be concerned mainly with renal studies (analysis of function of kidneys), however, the approach is applicable in other types of sequences as well.

The key problem of separation of activity of different organs in planar scintigraphy is that the activity from different organs is recorded by the same pixel in the scintigraphic image. From the camera point of view, the organ images overlap. One possible approach to overcome this difficulty is to manually select regions of interest (ROIs) [9], that marks pixels that are believed to belong to one organ only.

In nuclear medicine practice, methods based on the manual selection of the ROIs are mostly employed [5] which is, however, time consuming and prone to errors. There is a wide range of methods for automation of ROIs selection. User-independent approach using factor analysis, which separates structures automatically, has been presented in [14] and later in [4]. The segmentation of the whole kidney is studied in [8] while the automatic segmentation method that combines Fast Marching Method with Multi Agent System is proposed in [3] and its improved version in [2]. Recently, methods with the use of probability modeling have been proposed such as [11] favoring sparse solution or modeling specific behavior of time-activity curves [12]. Extensive study on modeling and estimation of time-activity curves has been given, e.g. in [6, 13].

In this paper, we follow up the probabilistic approach to modeling of scintigraphic sequences and estimation of the underlying source images and time-activity curves. Although the blind source separation step of the algorithm is automatic, we also consider the possibility of manual intervention of a user when the results are not anatomically correct. The manually selected ROIs should be used as a prior information to the separation method where an image signal should be suppressed or strengthened. The process can be iterated until an acceptable solution is found.

Performance of the presented approach is studied on dynamic medical sequences from the database of real data [1]. Specifically, we determine the relative renal function for the first 10 sequences and compare it to the results obtained by an experienced physician.

2 Mathematical Methods

Here, we will formulate a probabilistic model for blind and semi-supervised source separation of scintigraphic image sequence. We assume that the number of images in a sequence is n and each image consists of p pixels. The images are stored column-wise in columns of data matrix $D \in \mathbb{R}^{p \times n}$. Then the mathematical model of separation can be written as

$$D = AX^T + E, \tag{1}$$

where source images (i.e., individual physiological structures) are stored column-wise in columns of the matrix A, $A \in \mathbb{R}^{p \times r}$, associated flow of radioactive substances through these structures, called time-activity curves, are in columns of the matrix X, $X \in \mathbb{R}^{n \times r}$, and $E \in \mathbb{R}^{p \times n}$ is error matrix. The inner dimension of the product (1), r, is unknown. An upper bound on r has to be preselected for the studied problem, but the number of relevant sources will be determined automatically.

Our aim is to estimate unknown parameters of the model, A and X. We use Bayesian probability theory to do so since it allows to express our beliefs, assumptions and knowledge about parameters in the form of prior distributions. The prior distributions are then updated by the observed data.

2.1 Probabilistic Model

In (1), the model of each pixel $d_{i,j}$, $i = 1, ..., p$ and $j = 1, ..., n$, can be seen as the result of a product $\boldsymbol{a}_i^T$ and $\boldsymbol{x}_j$:

$$d_{i,j} = \boldsymbol{a}_i^T \boldsymbol{x}_j + e_{i,j}, \tag{2}$$

where $\boldsymbol{a}_i^T \in \mathbb{R}^{1 \times r}$ is i-th row of A, $\boldsymbol{x}_j \in \mathbb{R}^{r \times 1}$ is j-th column of X^T and $e_{i,j}$ associated element of E. We assume that $e_{i,j}$ is independently and identically Gaussian distributed as $f\left(e_{i,j}|\omega\right) = \mathcal{N}_{e_{i,j}}\left(0, \omega^{-1}\right)$, where $\mathcal{N}$ denotes Gaussian distribution with given mean and variance, and ω in the unknown variance of the noise common for all pixels, see [10] for details. Then the model of each data element $d_{i,j}$ can be written as

$$f\left(d_{i,j}|\boldsymbol{a}_i, \boldsymbol{x}_j, \omega\right) = \mathcal{N}_{d_{i,j}}\left(\boldsymbol{a}_i^T \boldsymbol{x}_j, \omega^{-1}\right), \tag{3}$$

$$f\left(\omega|\vartheta_0, \rho_0\right) = \mathcal{G}_{\omega}\left(\vartheta_0, \rho_0\right), \tag{4}$$

where $\mathcal{G}$ denotes Gamma distribution with prior parameters ϑ_0 and ρ_0. The parameters ϑ_0 and ρ_0 are assumed to be known with common choice being $\vartheta_0 = \rho_0 = 10^{-10}$ which correspond to non-informative prior. The Gamma prior is chosen because it is conjugate with unknown variance of Gaussian likelihood of $d_{i,j}$ (3). In nuclear medicine, each pixel $d_{i,j}$ is obtained as a count of radioactive particles and therefore $d_{i,j}$ is known to be Poisson-distributed and hence may be considered approximately Normal.

For model of A, we follow [12] and assume the pixel-element model as

$$f\left(a_{i,k}|\xi_{i,k}\right) = t\mathcal{N}_{a_{i,k}}\left(0, \xi_{i,k}^{-1}, [0, \infty)\right), \tag{5}$$

$$f\left(\xi_{i,k}|\phi_0, \psi_0\right) = \mathcal{G}_{\xi_{i,k}}\left(\phi_{0_{i,k}}, \psi_{0_{i,k}}\right), \tag{6}$$

where $t\mathcal{N}$ denotes truncated Gaussian distribution with given positive support and unknown precision hyperparameter $\xi_{i,k}$. The prior distribution for $\xi_{i,k}$ in (6) is chosen to favor sparse solution of the source images which is biologically motivated assumption since we assume that a tissue do not cover the whole area, see [12] for details. The prior parameters ϕ_0, ψ_0 are set to non-informative 10^{-10}. The prior model of elements of the time-activity curves is selected as $f(x_{j,k}) = t\mathcal{N}_{x_{j,k}}(0, 1, [0, \infty))$, where no specific assumption of time-activity curves has been made.

Since the exact determination of the model parameters is not tractable, we employ the variational Bayes method [10] to obtain approximate posterior densities which leads to a set of implicit equations that needs to be solved iteratively. This algorithm will be denoted as sparse blind source separation SparseBSS.

2.2 Semi-supervised Source Separation

After the run of the SparseBSS algorithm from Section 2.1, it could happen that some pixels that physiologically belong to one structure are incorrectly estimated to belong to another structure. We propose a way how to incorporate physiological information which could improve the resulting estimates. We exploit the possibility of modifying the prior parameters $\phi_{0_{i,k}}, \psi_{0_{i,k}}$ which can encourage the method to favor or not favor sparse solution in the selected regions. These prior parameters are influenced by manual intervention. They determine the shape of probability distribution of $\xi_{i,k}$ in (6) where $\xi_{i,k}$ is the inverse variance of pixel $a_{i,k}$. By setting the values of $\phi_{0_{i,k}}, \psi_{0_{i,k}}$ smaller than 10^{-10}, the Gamma distribution becomes flatter thus making larger values of $\xi_{i,k}$ more likely. Consequently, the inverse of $\xi_{i,k}$ can become smaller and therefore the estimate of $a_{i,k}$ is closer to zero. On the other hand, we can encourage higher values of pixel $a_{i,k}$ by setting the parameters $\phi_{0_{i,k}}, \psi_{0_{i,k}}$ larger than 10^{-10}. This process is summarized in Algorithm 1.

Algorithm 1 Proposed semi-supervised source separation algorithm.

1. Initialization:
   a. Set prior parameters $\vartheta_0, \rho_0, \phi_{0_{i,k}}, \psi_{0_{i,k}}$ to non-informative values 10^{-10}.
   b. Set assumed number of sources r.
2. Iterate until sufficient results are obtained:
   a. Run SparseBSS algorithm, Section 2.1.
   b. Perform manual selection of ROIs and assign new values of prior parameters $\phi_{0_{i,k}}, \psi_{0_{i,k}}$ in those ROIs.
3. Report estimates of A and X.

Selection of a ROI that should have different prior parameters is done by manual marking of its boundary. An example of the selected ROI as well as the graphical user interface can be seen in Fig. 1. The options for re-selection of prior parameters $\phi_{0_{i,k}}, \psi_{0_{i,k}}$ are 10^{-2} (suppressing pixels activity), 10^{-5}, 10^{-10}, 10^{-15} and 10^{-20} (encouraging picels activity). After the change in the selected ROIs, we apply the SparseBSS algorithm again. The process can be repeated until sufficient results are obtained. This stopping rule is subjective and for us it means repeat until the structures are separated from each other.

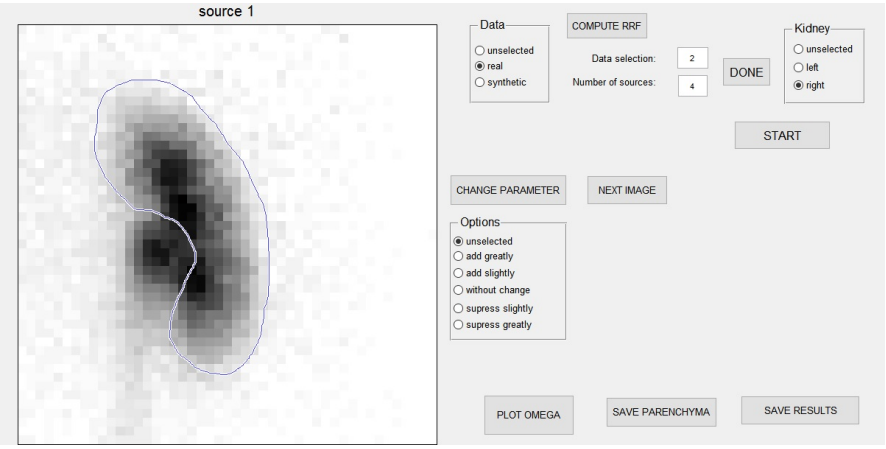

Fig. 1 Graphical user interface of the proposed semi-supervised source separation method. An example of manual ROI boundary drawing is displayed on the left.

3 Real Data Experiments

The derived probabilistic model was tested on real scintigraphic sequences from dynamic renal scintigraphy available from the online database [1]. Each sequence consists of 180 images taken repetitively every 10 seconds during dynamic scintigraphic examination. Each image has a dimension of 128×128 pixels. Since we will estimate relative renal function, we need to analyze each kidney separately. Hence, we select a square region of interest that contains the whole kidney surrounded by background and exclude the other kidney. Thus, it is possible to estimate the associated time-activity curves separately. The region can be placed manually and the size of the region is 47×47 pixels in all cases. Consequently, the dimension of the considered data matrix D is 2209×180.

First, we will demonstrate the separation on one selected sequence. Second, we will study the estimation of specific diagnostic parameter on a representative set of 10 sequences.

3.1 Selected Sequence Separation

We select one sequence to demonstrate the properties of the derived algorithm. The main task is to separate the sources, e.g., parenchyma, pelvis, and tissue background, from each other. For example, separation of parenchyma and pelvis is a very difficult task since the pelvis is surrounded by parenchyma which implicates that there are pixels corresponding to both parenchyma and pelvis. After applying radioactive substance into the human body, the first images detects activity of the tracer coming from the blood stream. Then comes the renal uptake phase in which the blood activity decreases and the activity of the parenchyma increases. So-called outflow phase follows when the parenchyma activity decreases and the activity of the pelvis increases. Eventually, the substance flows from pelvis into the urinary bladder.

We demonstrate the behavior of our method on the region with the right kidney. Every fifth image of this sequence is shown in Fig. 1.

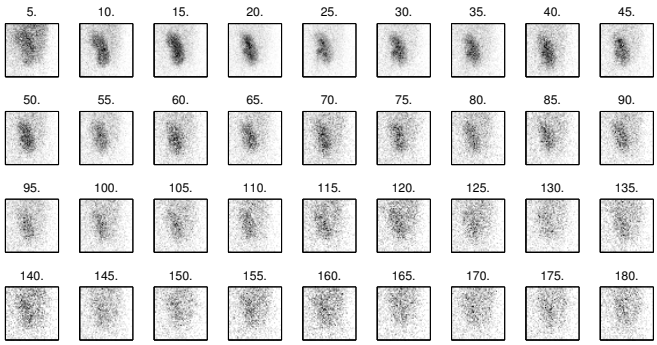

Fig. 1 Example scintigraphic image sequence where each 5th image is shown.

The inner dimension r is overestimated as 4 since we expect images to include at least activities from tissue background, parenchyma, and pelvis. Parameters ϕ_0 and ψ_0 were set equal to 10^{-10}. The results of the method is shown in Fig. 2, top panel. Evidently, our algorithm managed to separate the blood activity of the background (source 1) from the kidney (source 2). On the other hand, the algorithm was not able to separate the renal parenchyma from the pelvis. Source 3 represents residual pixels of the parenchyma and source 4

represents the noise with negligible activity during the whole dynamic renal scintigraphy.

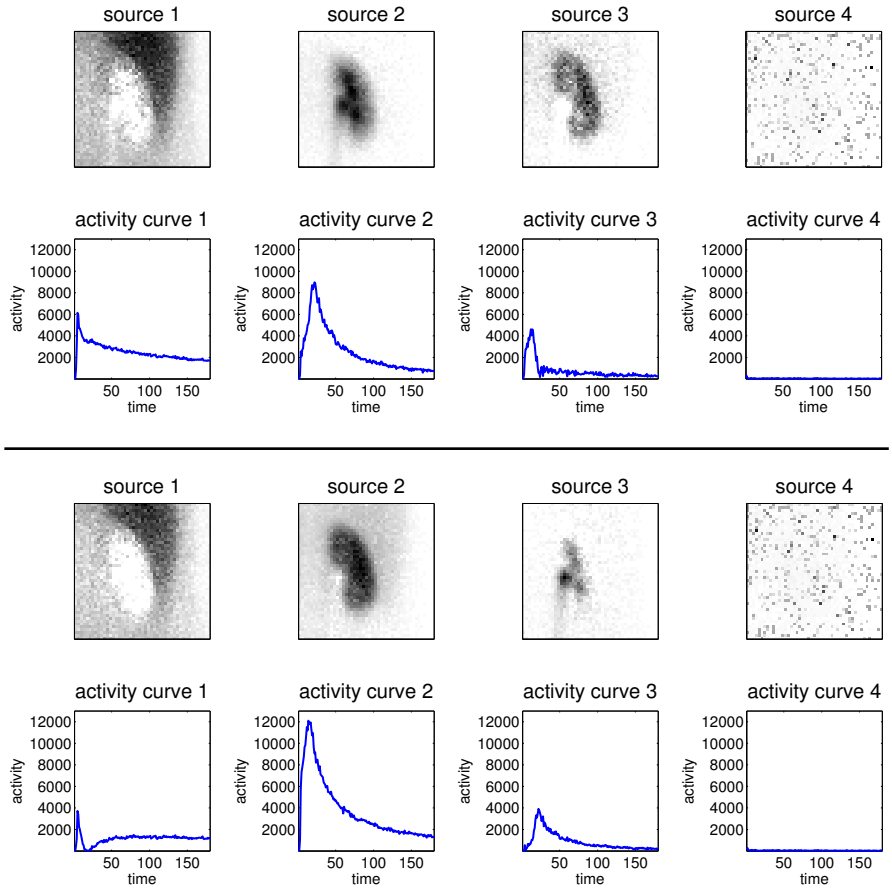

Fig. 2 Top panel: results of the SparseBSS algorithm. Bottom panel: Results of the SparseBSS algorithm after manual intervention.

In order to obtain pelvis as an individual factor, we try to suppress pixels of parenchyma in source 2 by setting parameters ϕ_0 and ψ_0 equal to 10^{-15}. The mask of pixels, where these parameters were changed can be seen in Fig. 3. The results of the second run of the algorithm are shown in Fig. 2, bottom panel. In this case, the method was able to estimate tissue background activity (source 1) and parenchyma (source 2) as individual factors and simultaneously separate pelvis (source 3) from parenchyma. The consequence is that their time-activity curves are also well separated.

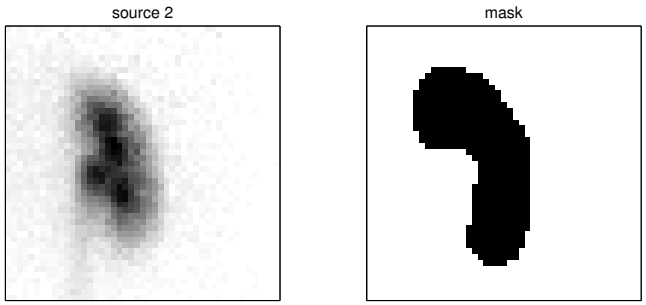

Fig. 3 Source 2 (left) and mask of suppressed pixels (right).

3.2 Relative Renal Function Estimation

In our experiment, the relative renal function (RRF) will be estimated and compared to the values obtained by a physician which are also included in the database. The RRF is generally determined from the parenchyma and its associated time-activity curves as the relative activity of the left and the right parenchyma. The consensus is that only first 12 images (i.e., 2 minutes) of the scintigraphy sequence are used [7] where no other activities then from parenchyma and background are typically present. It is usually called the uptake phase of the sequence. The RRF can be computed as

$$RRF = \frac{S_A^L \cdot S_X^L}{S_A^L \cdot S_X^L + S_A^R \cdot S_X^R} \cdot 100\ [\%]\,, \tag{7}$$

where S_A denotes the sum of a column of the matrix A which is associated with the estimate of the parenchyma. Analogously, S_X denotes the sum of a row of the matrix X which belongs to the estimate of the activity curve for the parenchyma. Upper indexes L and R denote left and right parenchyma respectively.

The first 10 sequences from the database ([1], note that we preserve sequences numbering from [1] where the sequence number 3 is missing) were chosen for the experimental purposes in order to estimate the RRF. The results obtained using the equation (7) after applying the derived algorithm are compared with those determined by the physician in Tab. 1. In six cases out of ten, the difference is smaller than 3% and in other four cases the difference is greater than 10% (sequences 4, 5, 6 and 9). As the next step, we try to improve the estimates of parenchyma of both kidneys to get even more accurate values of RRF by manual selection of regions, where prior parameters ϕ_0 and ψ_0 should be changed. The results after manual intervention and the

second cycle of the algorithm are also summarized in Tab. 1. It is apparent that in these four cases, we were able to significantly enhance the estimate. Nonetheless, some estimates of RRF that were close to those chosen by physician before manual intervention are now a little bit worse but the difference is still less than 6%.

	Relative renal function [%]		
	by physician	after first run of SparseBSS	after manual intervention
Sequence 1	62	59	59
Sequence 2	52	49	46
Sequence 4	57	70	63
Sequence 5	87	70	76
Sequence 6	18	39	30
Sequence 7	51	52	53
Sequence 8	39	37	40
Sequence 9	24	54	17
Sequence 10	54	52	59
Sequence 11	18	18	21

Table 1 Comparison of the estimated relative renal function.

To conclude, changing of parameters ϕ_0 and ψ_0 which influence the variance of individual pixels in manually selected areas can improve the estimation of the sources and corresponding time-activity curves.

4 Conclusion

In this contribution, we presented a new method for semi-supervised source separation of dynamic medical image sequences. We use the factor analysis model together with Bayesian approach where parameters of the model are considered as unknown variables to be estimated using the variational Bayes method. We allow manual intervention of the user by selecting regions of interest and changing parameters of the prior distribution. The user can increase or decrease the probability that the region belong to that source. The same algorithm is run again with modified prior information.

The usefulness of the method is demonstrated on selected real medical image sequence where improved separation is shown. Moreover, the method is used to estimate relative renal function on a set of 10 sequences. Here, we observe that the results of the basic method can be significantly improved

using proposed manual intervention and incorporation into the estimating procedure.

Acknowledgements This work was supported by the Grant Agency of the Czech Technical University in Prague, grant No. SGS17/193/OHK4/3T/14.

References

1. Database of dynamic renal scintigraphy http://dynamicrenalstudy.org. accessed: 2017-02-28.
2. Y. Aribi, F. Hamza, A. Wali, A. M. Alimi, and F. Guermazi. An automated system for the segmentation of dynamic scintigraphic images. *Applied Medical Informatics*, 34(2):1, 2014.
3. Y. Aribi, A. Wali, and A. M. Alimi. An intelligent system for renal segmentation. In *e-Health Networking, Applications & Services (Healthcom), 2013 IEEE 15th International Conference on*, pages 11–15. IEEE, 2013.
4. H. Bergmann, E. Dworak, B. König, A. Mostbeck, and M. Šámal. Improved automatic separation of renal parenchyma and pelvis in dynamic renal scintigraphy using fuzzy regions of interest. *European Journal of Nuclear Medicine and Molecular Imaging*, 26(8):837–843, 1999.
5. M. Caglar, G.K. Gedik, and E. Karabulut. Differential renal function estimation by dynamic renal scintigraphy: influence of background definition and radiopharmaceutical. *Nuclear Medicine Communications*, 29(11):1002–1005, 2008.
6. L. Chen, P.L. Choyke, T.-H. Chan, C.-Y. Chi, G. Wang, and Y. Wang. Tissue-specific compartmental analysis for dynamic contrast-enhanced MR imaging of complex tumors. *IEEE Transactions on Medical Imaging*, 30(12):2044–2058, 2011.
7. E. Durand, M.D. Blaufox, K.E. Britton, O. Carlsen, P. Cosgriff, E. Fine, J. Fleming, C. Nimmon, A. Piepsz, A. Prigent, et al. International Scientific Committee of Radionuclides in Nephrourology (ISCORN) consensus on renal transit time measurements. In *Seminars in Nuclear Medicine*, volume 38, pages 82–102. Elsevier, 2008.
8. E. V. Garcia, R. Folks, S. Pak, and A. Taylor. Totally automatic definition of renal regions-of-interest from tc-99m mag3 renograms: Validation in patients with normal kidneys and in patients with suspected renal obstruction. *Nuclear Medicine Communications*, 31(5):366, 2010.
9. R. S. Lawson. Application of mathematical methods in dynamic nuclear medicine studies. *Physics in Medicine and Biology*, 44(4):R57, 1999.
10. V. Šmídl and A. Quinn. *The variational Bayes method in signal processing*. Springer Science & Business Media, 2006.
11. V. Šmídl and O. Tichý. Automatic regions of interest in factor analysis for dynamic medical imaging. In *Biomedical Imaging (ISBI), 2012 9th IEEE International Symposium on*, pages 158–161. IEEE, 2012.
12. O. Tichý and V. Šmídl. Bayesian blind separation and deconvolution of dynamic image sequences using sparsity priors. *IEEE Transactions on Medical Imaging*, 34(1):258–266, 2015.
13. O. Tichý and V. Šmídl. Non-parametric Bayesian models of response function in dynamic image sequences. *Computer Vision and Image Understanding*, 151:90–100, 2016.
14. M. Šámal, C. C. Nimmon, K. E. Britton, and H. Bergmann. Relative renal uptake and transit time measurements using functional factor images and fuzzy regions of interest. *European Journal of Nuclear Medicine and Molecular Imaging*, 25(1):48–54, 1998.